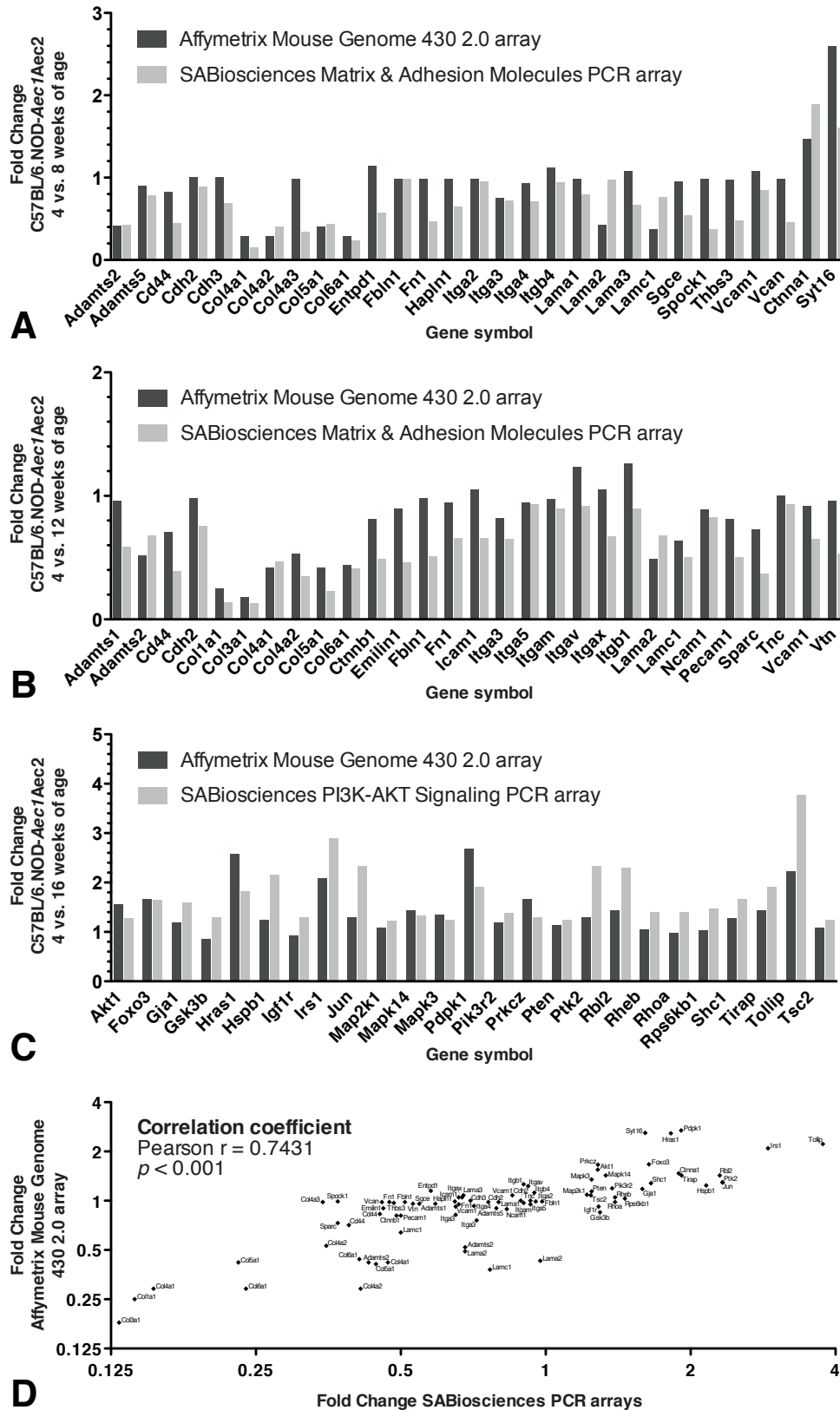


Additional file 1

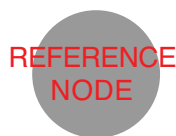
Figure S1)



Comparing fold changes in gene expression over time inferred from microarray and real-time PCR data. A-C) Fold changes in gene expression as yielded by the SABiosciences Extracellular Matrix & Adhesion Molecules PCR array and SABiosciences PI3K-AKT Signaling PCR array, respectively compared to fold changes computed based on the Affymetrix 3' Expression Array GeneChip Mouse Genome 430 2.0 array data. **D)** Scatter plot of the data displayed in Supplementary Figures 1A-1C. Statistical analyses demonstrate a significant correlation between the fold changes obtained with the two methods (Pearson $r = 0.7431$; $p < 0.001$).

Figure S2)

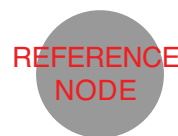
1) Collagen I & III



A

GO_0005581
(COLLAGEN)

1) Collagen I & III



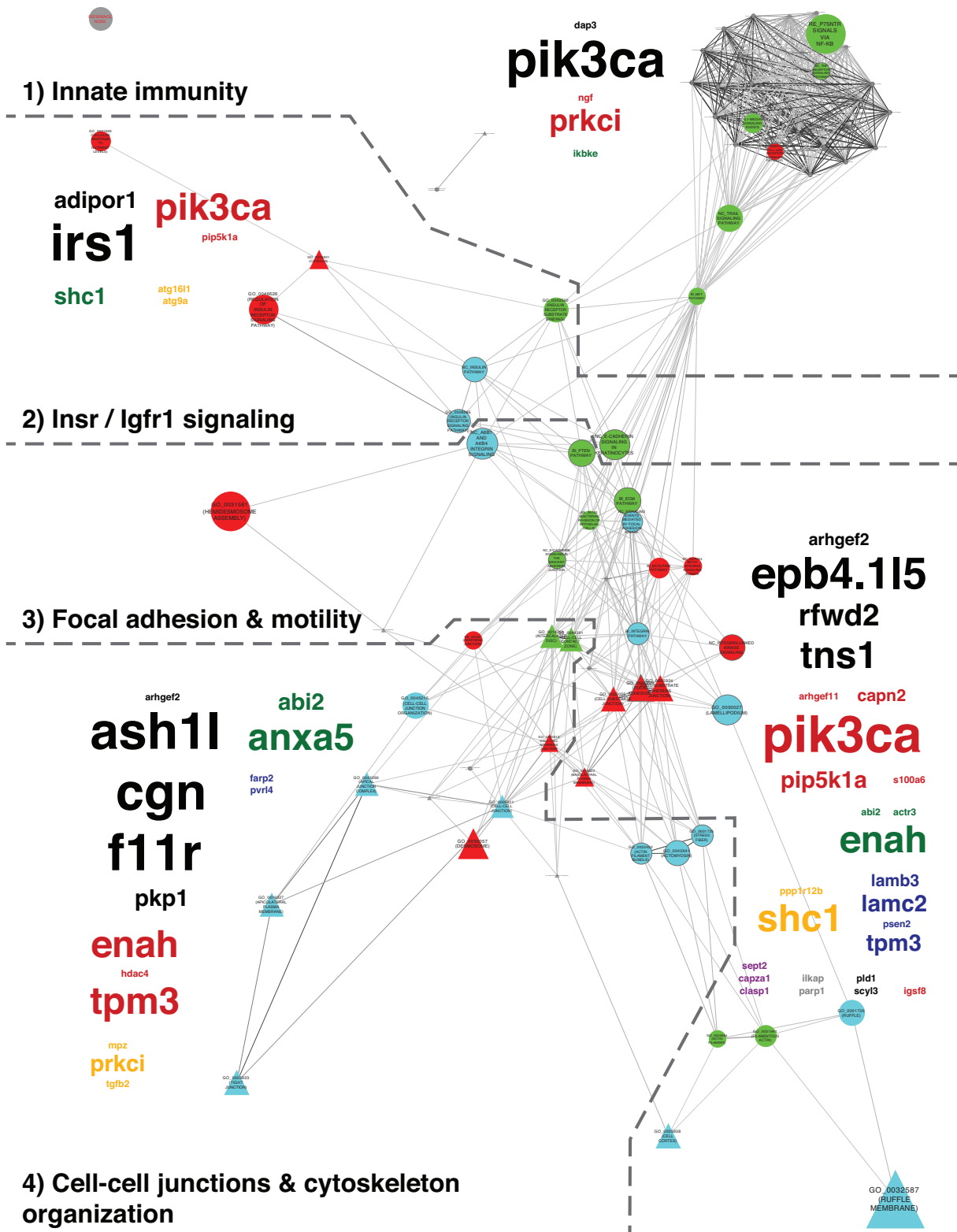
B

col11a2
col1a1
col1a2
col3a1
col4a1
col4a2
col4a4
col4a5
col5a2
col9a1

lox GO_0005581
tnxb (COLLAGEN)

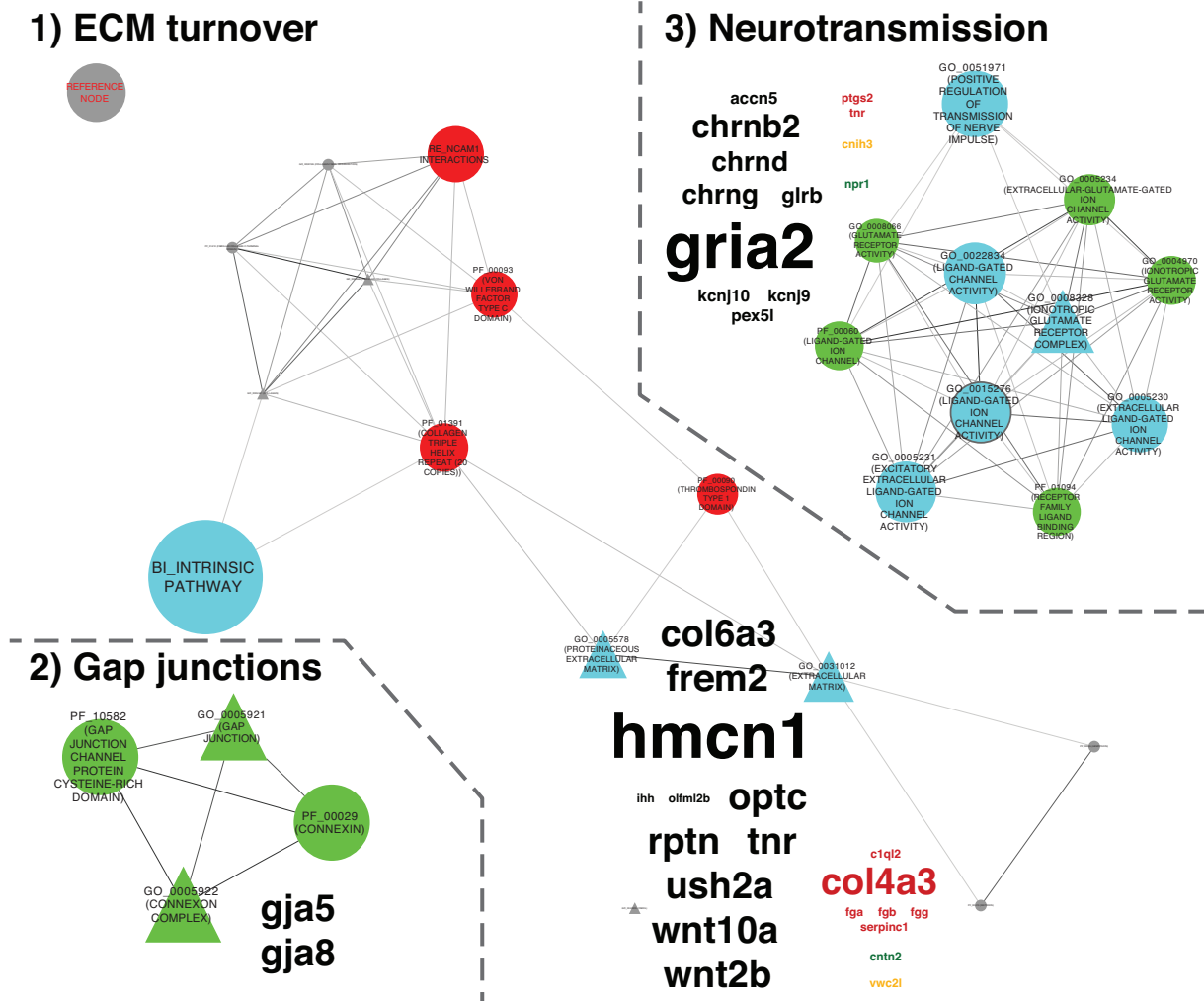
Stabilization of the subclinical disease state in C57BL/6.NOD-*Aec1Aec2* mice between 8 and 12 weeks of age. GO_0005581 (COLLAGEN) was the only GS, which yielded significance during this time period by continuing its depletion initiated between 4 and 8 weeks of age already. The LE-genes indicate collagen I & III to be important. **A)** The layout parameters of Figure S2A correspond precisely to the layout parameters of Figure 3. The reference node allows estimation of scaling and direct comparison of Figures 3, 5A, 6A, 7A & Figure S2A. **B)** Annotation of the GS displayed in Figure S2A with its respective LE-gene cloud. The layout parameters of Figure S2B correspond precisely to the layout parameters of Figure 4. The reference node allows estimation of scaling and direct comparison of Figures 4, 5B, 6B, 7B & Figure S2B. Figure infinitely scalable and electronically searchable.

Figure S3)



Contributions of genes located in susceptibility regions *Aec1* and *Aec2* to enrichments in the EM's transcriptional landscape during transition from pre- to subclinical SS in C57BL/6.NOD-*Aec1Aec2* mice between 4 and 8 weeks of age. Dashed line = separator between the major biological themes; **Node color: green = LE-genes located in *Aec1*; red = LE-genes located in *Aec2*, blue = LE-genes located in both congenic regions, grey = no LE-genes located in *Aec1* or *Aec2*; **node size and node label font size** = proportional to the percentage of LE-genes located in the congenic regions (Reference Node = 10%); **node shape:** triangular = EM-related, circular = EM-associated; **node border:** none = alteration of this GS exclusive to C57BL/6.NOD-*Aec1Aec2* mice, present = reciprocal trend in C57BL/6 mice. **Edge color** = degree of overlap in LE-genes between the two GSs connected by this edge. **Clustered LE-gene clouds: Font color** = clustering of the LE-genes located in the susceptibility regions based on the connections between the GSs of the respective major biological theme; **font size** = frequency of this gene in the LEs of the GSs combined in the respective major biological theme. Figure infinitely scalable and electronically searchable.**

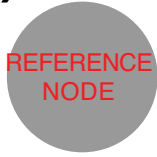
Figure S4)



Contributions of genes located in susceptibility regions *Aec1* and *Aec2* to depletions in the EM's transcriptional landscape during transition from pre- to subclinical SS in C57BL/6.NOD-*Aec1Aec2* mice between 4 and 8 weeks of age. The layout parameters of Figure S4 correspond precisely to the layout parameters of Figure S3. The reference node allows estimation of scaling and direct comparison of Supplementary Figures 3-7. Figure infinitely scalable and electronically searchable.

Figure S5)

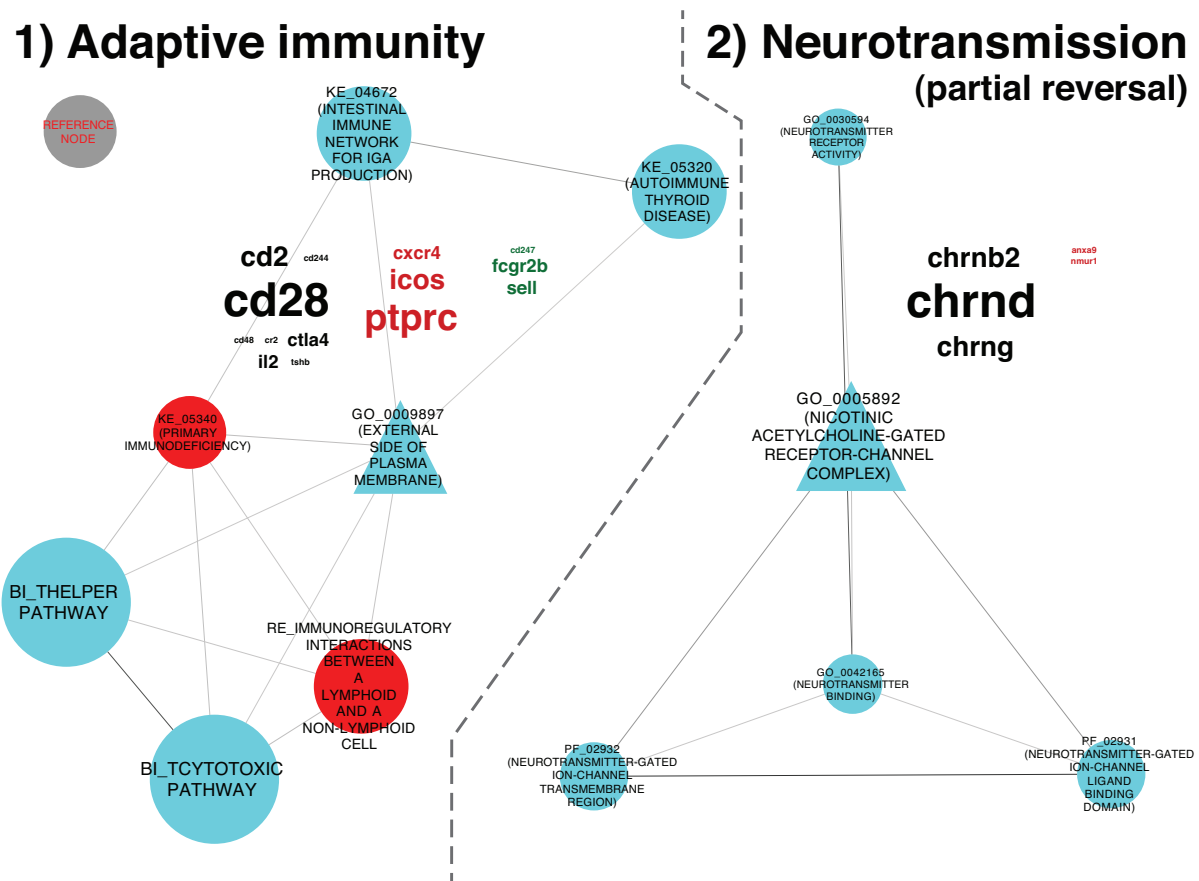
1) Collagen I & III



col4a4
GO_0005581
(COLLAGEN)

Contribution of genes located in the susceptibility regions *Aec1* and *Aec2* to the stabilization of the subclinical disease state in C57BL/6.NOD-*Aec1Aec2* mice between 8 and 12 weeks of age. The layout parameters of Figure S5 correspond precisely to the layout parameters of Figure S3. The reference node allows estimation of scaling and direct comparison of Supplementary Figures 3-7. Figure infinitely scalable and electronically searchable.

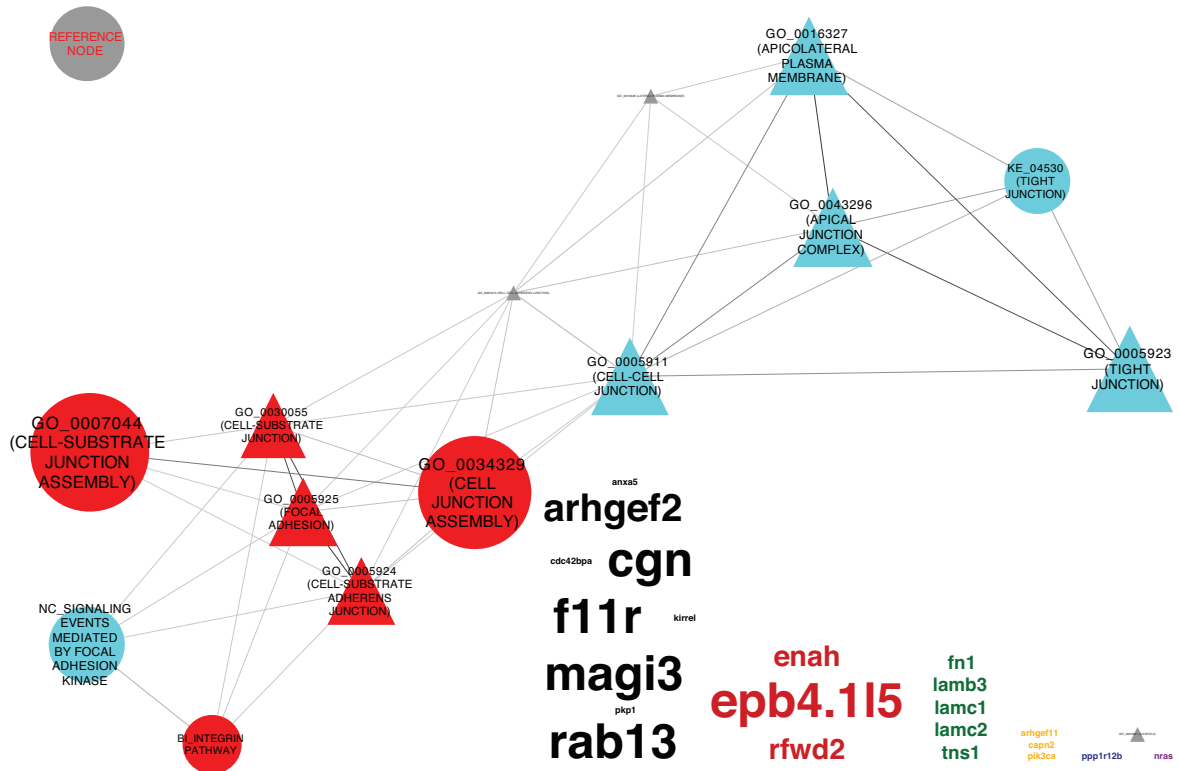
Figure S6)



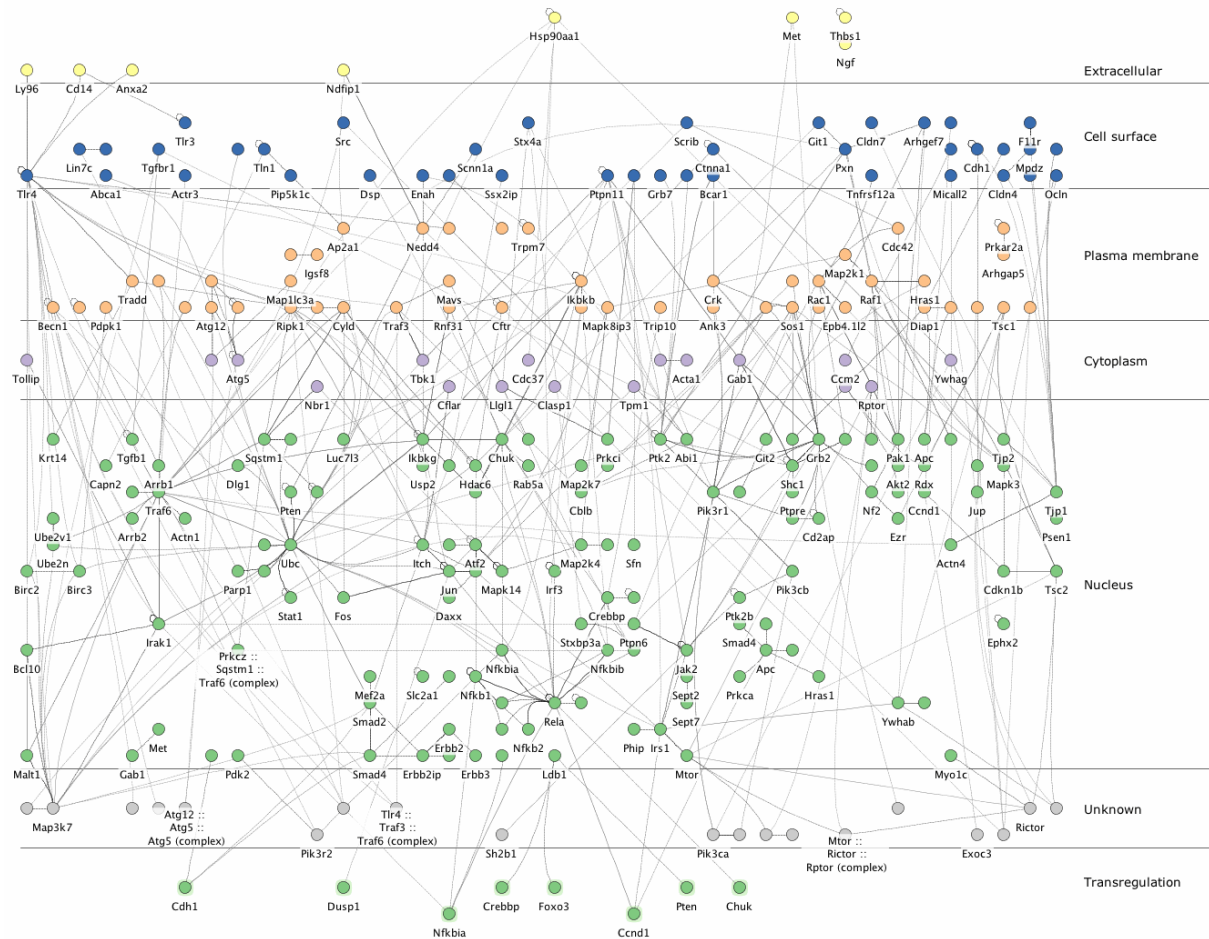
Contributions of genes located in susceptibility regions *Aec1* and *Aec2* to enrichments in the EM's transcriptional landscape during transition from subclinical to overt SS in C57BL/6.NOD-*Aec1Aec2* mice between 12 and 16 weeks of age. The layout parameters of Figure S6 correspond precisely to the layout parameters of Figure S3. The reference node allows estimation of scaling and direct comparison of Supplementary Figures 3-7. Figure infinitely scalable and electronically searchable.

Figure S7)

1) Focal adhesion & cell-cell junctions (partial reversal)



Contributions of genes located in susceptibility regions *Aec1* and *Aec2* to depletions in the EM's transcriptional landscape during transition from subclinical to overt SS in C57BL/6.NOD-*Aec1Aec2* mice between 12 and 16 weeks of age. The layout parameters of Figure S7 correspond precisely to the layout parameters of Figure S3. The reference node allows estimation of scaling and direct comparison of Supplementary Figures 3-7. Figure infinitely scalable and electronically searchable.

Figure S8)

Cell Region-Based Rendering And Layout (Cerebral) [1] of an interactome model based on the LE-members associated with enrichments in the EM's transcriptional landscape during transition from pre- to subclinical SS in C57BL/6.NOD-*Aec1Aec2* mice between 4 and 8 weeks of age (Figure 3 & 4). Mining of the experimental data was computed using InnateDB [2]. **Line opacity = strength of experimental evidence; **node color** = subcellular localization (not curated).**

Supplementary References

1. Barsky A, Gardy JL, Hancock RE, Munzner T: **Cerebral: a Cytoscape plugin for layout of and interaction with biological networks using subcellular localization annotation.** *Bioinformatics* 2007, **23**(8):1040-1042.
2. Lynn DJ, Winsor GL, Chan C, Richard N, Laird MR, Barsky A, Gardy JL, Roche FM, Chan TH, Shah N *et al*: **InnateDB: facilitating systems-level analyses of the mammalian innate immune response.** *Mol Syst Biol* 2008, **4**:218.